Journal of Biomechanics 144 (2022) 111306

Contents lists available at ScienceDirect

Journal of Biomechanics

journal homepage: www.elsevier.com/locate/jbiomech

Interpretation of natural tibio-femoral kinematics critically depends upon the kinematic analysis approach: A survey and comparison of methodologies

Barbara Postolka [a,*], William R. Taylor [a], Katrin Dätwyler [a], Markus O. Heller [b], Renate List [a,c], Pascal Schütz [a]

[a] Institute for Biomechanics, ETH Zürich, Zürich, Switzerland
[b] Mechanical Engineering Unit, Engineering and the Environment, University of Southampton, Southampton, United Kingdom
[c] Human Performance Lab, Schulthess Clinic, Zürich, Switzerland

ARTICLE INFO

Keywords:
in vivo knee kinematics
fluoroscopy
movement and motion analysis
centre of rotation
antero-posterior translations

ABSTRACT

While there is general agreement on the transverse plane knee joint motion for loaded flexion activities, its kinematics during functional movements such as level walking are discussed more controversially. One possible cause of this controversy could originate from the interpretation of kinematics based on different analysis approaches. In order to understand the impact of these approaches on the interpretation of tibio-femoral motion, a set of dynamic videofluoroscopy data presenting continuous knee bending and complete cycles of walking in ten subjects was analysed using six different kinematic analysis approaches. Use of a functional flexion axis resulted in significantly smaller ranges of condylar translation compared to anatomical axes and contact approaches. All contact points were located significantly more anteriorly than the femur fixed axes after 70° of flexion, but also during the early/mid stance and late swing phases of walking. Overall, a central to medial transverse plane centre of rotation was found for both activities using all six kinematic analysis approaches, although individual subjects exhibited lateral centres of rotation using certain approaches. The results of this study clearly show that deviations from the true functional axis of rotation result in kinematic crosstalk, suggesting that functional axes should be reported in preference to anatomical axes. Contact approaches, on the other hand, can present additional information on the local tibio-femoral contact conditions. To allow a more standardised comparison and interpretation of tibio-femoral kinematics, results should therefore be reported using at least a functionally determined axis and possibly also a contact point approach.

1. Introduction

Accurate assessment of tibio-femoral kinematics in both healthy and pathological joints is essential for the quantification and understanding of knee joint functionality (Asano et al., 2005; Freeman and Pinskerova, 2005) but also for developing joint prostheses (Banks et al., 1996; Schütz et al., 2019). The motion of the knee joint is characterized by a complex combination of flexion/extension together with internal/external rotation and antero-posterior (A-P) translation of the femoral condyles relative to the tibia (Andriacchi et al., 1998). To describe this time-dependent three-dimensional (3D) motion, a variety of kinematic analysis approaches based on different segment proximity measures, coordinate systems, and/or axes of rotation, have been proposed. These approaches can generally be categorized into three groups: contact estimates, functional axes, and anatomical axes (Table 1). Based on the resulting medial and lateral condylar A-P translations, the tibio-femoral centre of rotation (CoR) in the transverse plane can then be determined using either least-squares approaches (Banks and Hodge, 2004; Gray et al., 2019), sphere fitting (Gamage and Lasenby, 2002), or transformation techniques (Ehrig et al., 2006; Holzreiter, 1991). Application of these kinematic analysis approaches to bone poses captured using magnetic resonance imaging (MRI) (Vedi et al., 1999) or videofluoroscopy (Dennis et al., 2001; Galvin et al., 2019; Guan et al., 2016; Kozanek et al., 2009; Li et al., 2008; List et al., 2017; Moro-oka et al.,

* Corresponding author at: ETH Zürich, Laboratory for Movement Biomechanics, Institute for Biomechanics, Leopold-Ruzicka-Weg 4, CH - 8093 Zürich, Switzerland.
E-mail address: barbara.postolka@hest.ethz.ch (B. Postolka).

https://doi.org/10.1016/j.jbiomech.2022.111306
Accepted 12 September 2022
Available online 17 September 2022

Table 1
Summary of kinematic analysis approaches used in the literature.

Kinematic Analysis Approaches		
Contact Estimates	Contact Region	Centroid of the area formed by the overlap of the femoral and tibial cartilage (DeFrate et al., 2004)
	Nearest Points (NP)	Nearest points of each femoral condyle relative to the tibia (Asano et al., 2001; Dennis et al., 2005)
	Lowest Points	Lowest points of each femoral condyle in the tibial coordinate system (Grieco et al., 2018)
	Tibio-Femoral Separation (SEP)	Geometric centre of the region having less tibio-femoral separation then a certain threshold (Moro-oka et al., 2008)
Functional Axes	Functional Axis of Rotation	Derived from the relative movement of the femur and tibia. - Least squares estimates (Asano et al., 2005; Gamage and Lasenby, 2002) - Mean helical axis (Besier et al., 2003) - Symmetrical axis of rotation approach (SARA) (Ehrig et al., 2007; Ehrig and Heller, 2019)
Anatomical Axes	Transepicondylar Axis (TEA)	Connection of the most prominent points of the medial and lateral epicondyle (Berger et al., 1993; Churchill et al., 1998)
	Geometric Centre Axis (GCA) / Circular Axis (CA)	Based on the fitting of circular, cylindrical or spherical shapes to the femoral condyles (Asano et al., 2001; Eckhoff et al., 2001; Kurosawa et al., 1985)
	Extension Facet Centre (EFC) / Flexion Facet Centre (FFC)	Anterior and posterior circular surfaces of the femur that are in contact with the tibia during certain phases of knee flexion (Iwaki et al., 2000)

2008) are able to provide access to the tibio-femoral joint motions in all degrees of freedom. However, while a general understanding of knee joint movement patterns has been achieved, including scientific and clinical agreement on the physiological range of A-P translation of the medial versus the lateral condyle as well as the location of the CoR during loaded knee flexion (Table 2), tibio-femoral kinematics during functional activities such as level walking remain controversially discussed (Table 3).

For loaded knee flexion activities (Table 2), the lateral condyle shows an overall larger A-P translation compared to the medial condyle for analysis using anatomical axes (Asano et al., 2005, 2001; Hill et al., 2000; Johal et al., 2005; Pinskerova et al., 2004; Tanifuji et al., 2013, 2011) as well as contact estimates (Asano et al., 2001; DeFrate et al., 2004; Dennis et al., 2005, 2001; Hamai et al., 2013; Komistek et al., 2003; Li et al., 2005; Moro-oka et al., 2008; Yamaguchi et al., 2009). In addition, analysis of contact estimates has also resulted in almost equal translations for the two condylar points (Grieco et al., 2018; Li et al., 2006; Pinskerova et al., 2004; Qi et al., 2013). For functional movements such as level walking (Table 3), a medial CoR, indicating more A-P translation of the lateral compared to the medial compartment, was found using contact points (Dennis et al., 2001) but also geometrical (Gray et al., 2019) as well as functional axes (Postolka et al., 2020b). Controversially, larger medial than lateral A-P translations were found using a geometrical and transepicondylar axis, as well as cartilage contact measures (Kozanek et al., 2009; Liu et al., 2010), which are supported by the lateral CoR observed by Koo & Koo (2019).

More than basic differences between study conditions (e.g. patient characteristics, task, measurement technique etc.), it is entirely conceivable that the different kinematic analysis approach and convention used for reporting study outcomes may have led to misunderstandings and contradictory conclusions of what are, in fact, similar motion patterns. Previous studies have indeed compared different kinematic analysis approaches *in vitro* (Eckhoff et al., 2007; Most et al., 2004; Walker et al., 2011) during simulated movements and *in vivo* (Feng et al., 2016; Gray et al., 2019; Kozanek et al., 2009; Postolka et al., 2020b; Tanifuji et al., 2013) during functional activities. Despite consensus that femoral condylar motion is sensitive to the definition of femur fixed axes (Feng et al., 2016; Most et al., 2004), a comprehensive comparison of condylar motion using femur fixed axes and contact estimates during both loaded knee flexion and functional gait activities *in vivo* is missing. Therefore, this study aimed to compare the impact of six different kinematic analysis approaches on the interpretation of transverse plane knee joint motion based on a set of consistent dynamic videofluoroscopic data during deep knee bending and level walking.

2. Materials & methods

2.1. Tibio-femoral data capture

Kinematic data was acquired for ten healthy subjects (5 female/5 male, aged 23.7 ± 3.2 years, BMI 21.7 ± 2.2 kg/m^2, hip-knee-ankle angle 0.6 ± 1.4° varus) during standing (2 trials), continuous knee flexion (step down activity of the contralateral limb, whereby the tested knee underwent full extension to maximum flexion, 3 trials) as well as complete cycles of level walking (5 – 6 trials) using a dynamic videofluoroscope (List et al., 2017). A detailed description of the motion tasks and the measurement procedure has been published previously (Postolka et al., 2020b), however a brief description is provided here: Single-plane videofluoroscopic images were captured at 25 Hz (1 ms shutter time, 1000x1000 pixels image resolution) in combination with ground reaction force data (2000 Hz) using five force plates (Kistler AG, Switzerland). The vertical ground reaction force was used to define heel-strike and toe-off during level walking (threshold 25 N). In order to perform 2D/3D registration of the fluoroscopic images, a CT scan of each subject's knee (~20 cm proximal/distal of the joint space, resolution 0.5x0.5 mm, slice thickness 1 mm) was manually segmented to generate subject-specific femoral and tibial models (mean point separation 0.4 mm) (Pauchard et al., 2016). Semi-automatic 2D/3D registration was then performed using an in–house software, resulting in registration errors of <0.6 mm for in-plane translations, <7.1 mm for out-of-plane translations and <1° for all rotations (Postolka et al., 2020a). All subjects provided written, informed consent to participate in this study, which was approved by the local ethics committee (KEK-ZH-Nr. 2016-00410).

2.2. Kinematic analyses

In order to obtain physiological segment rotations, local femoral and tibial anatomical coordinate systems were defined (Postolka et al., 2020b) and tibio-femoral rotations were calculated according to Grood and Suntay (1983). To define a plane parallel to the tibial articular surface, an initial vector was constructed to describe the tibial slope in the sagittal plane. A second vector, completing the definition of the plane, was defined orthogonal to the initial vector and aligned with the medio-lateral slope. Condylar A-P translations were analysed using six different kinematic analysis approaches (Table 4). To consistently describe condylar motion across all approaches, the medial and lateral femoral points of the functional flexion axis (FFA), the transepicondylar axis (TEA), and the cylinder axis (CA), were defined as the intersection of the axes with a medial and lateral sagittal plane fitted through the nearest points (NP) during standing. Per definition, the tibio-femoral separation (SEP) points and the extension facet centre and flexion facet centre (EFC/FFC) points were also defined in the same medial and lateral sagittal planes. A-P translation of each femoral condyle was then

Table 2
Summary of antero-posterior translation and the centre of rotation (CoR) during loaded knee flexion using different approaches.

	Author	# Knees (age)	Imaging Modality	RoM evaluated	Method	A-P Translation		CoR
						Medial	Lateral	
Loaded Knee Flexion	Asano et al., 2001	6 (25 – 43 years)	biplane X-ray	0 – 120°	GCA	3.8 mm a	17.8 mm p	medial
					NP	0 – 30°: 6.9 mm p	0 – 120°: 27.4 mm p	medial
	Asano et al., 2005	9 (25 – 43 years)	biplane X-ray	0 – 90°	FFA	n.a.	n.a.	medial
	DeFrate et al., 2004	5 (21 – 41 years)	dual-plane fluoroscopy	0 – 90°	NP	4.5 ± 3.3 mm p	13.3 ± 5.7 mm p	n.a.
	Dennis et al., 2001	5	single-plane fluoroscopy	0 – 90°	CP	n.a.	n.a.	medial
	Dennis et al., 2005	10 (22 – 44 years)	single-plane fluoroscopy	0 – 120°	NP	1.9 ± 1.9 mm p	21.1 ± 9.3 mm p	n.a.
	Grieco et al. 2018	10 (57.4 ± 7.1 years)	single-plane fluoroscopy	0 – 120°	NP	0 – 30°: 4.7 ± 2.2 mm p 30 – 60°: 0.2 ± 1.1 mm p 60 – 90°: 0.4 ± 2.2 mm a 90 – 120°: 0.6 ± 1.6 mm a	0 – 30°: 11.8 ± 4.4 mm p 30 – 60°: 3.2 ± 2.8 mm p 60 – 90°: 1.4 ± 2.7 mm p 90 – 120°: 3.4 ± 5.1 mm p	n.a.
	Hamai et al., 2013	5 (28 – 30 years)	single-plane fluoroscopy	85 – 150°	CP	2 mm p	8 mm p	medial
	Hill et al., 2000	7 (22 – 35 years)	MRI	-5 – 90°	FFC/ EFC	10 – 90°: 4 mm a	p	n.a.
	Johal et al., 2005	10 (20 – 30 years)	MRI	-5 – 140°	FFC/ EFC	-5 – 90°: 2.2 ± 1.5 mm a 90 – 120°: 3.6 ± 2.0 mm p 120 – 140°: 9.4 ± 2.1 mm p	-5 – 120°: 21.1 ± 4.7 mm p 120 – 140°: 9.8 ± 2.1 mm p	medial
	Komistek et al., 2003	4 (29 – 44 years)	single-plane fluoroscopy	0 – 90°	CP	1.5 mm p (3.0 mm a – 4.6 mm p)	14.1 mm p (5.8 – 24.7 mm p)	medial
	Li et al., 2005	5 (25 ± 5 years)	dual-plane fluoroscopy	0 – 90°	CP	~1.5 mm p	~9mm p	n.a.
	Li et al., 2006	9 (19 – 38 years)	dual-plane fluoroscopy	0 – 90°	CP	11.1 ± 2.4 mm p	11.8 ± 4.3 mm p	n.a.
	Moro-oka et al., 2008	6 (28 – 31 years)	single-plane fluoroscopy	0 – 150°	NP	p	p	>80°: medial
	Pinskerova et al., 2004	5	MRI	-5 – 120°	FFC/ EFC	no movement	20 mm p	medial
					CP	19 mm p	22 mm p	n.a.
	Qi et al., 2013	8 (23 – 49 years)	dual-plane fluoroscopy	-5 – 150°	CP	11.1 ± 3.3 mm p	14.6 ± 3.7 mm p	n.a.
	Tanifuji et al., 2011	20 (24 – 61 years)	single-plane fluoroscopy	0 – 140°	GCA	0 – 100°: 5.5 ± 3.7 mm a 100 – 140°: 3.9 ± 2.9 mm p	0 – 140°: 15.6 ± 5.0 mm p	0 – 120°: medial
	Tanifuji et al., 2013	20 (24 – 61 years)	single-plane fluoroscopy	0 – 140°	TEA	0 – 30°: 3.6 ± 3.0 mm a 30 – 140°: 18.1 ± 3.7 mm p	0 – 140°: 31.7 ± 7.3 mm p	n.a.
	Yamaguchi et al., 2009	8 (41 ± 7 years)	single-plane fluoroscopy	-10 – 110°	CP	n.a.	n.a.	medial

A-P: antero-posterior, CoR: centre of rotation, RoM: range of motion, a: anterior, p: posterior
GCA: geometric centre axis, FFC: flexion facet centre, EFC: extension facet centre, FFA: functional flexion axis, TEA: transepicondylar axis, NP: nearest point, CP: contact point

Table 3
Summary of antero-posterior translation and the centre of rotation (CoR) during level walking using different approaches.

	Author	# Knees (age)	Imaging Modality	Phase of Gait	Method	A-P Translation		CoR
						Medial	Lateral	
Level Walking	Dennis et al., 2001	5	single-plane fluoroscopy	stance	CP	0.8 mm	7.3 mm	medial
	Gray et al., 2019	15 (30.5 ± 6.2 years)	dual-plane fluoroscopy	stance & swing	GCA NP	7.6 mm 9.7 mm	11.6 mm 15.4 mm	medial n.a.
	Komistek et al., 2003	4 (29 – 44 years)	single-plane fluoroscopy	stance	CP	0.9 mm a (5.9 mm a – 3.4 mm p)	4.3 mm p (1.9 – 10.3 mm p)	n.a.
	Koo and Koo, 2019	7 (23 ± 2 years)	dual-plane fluoroscopy	mid swing – mid stance	CP	n.a.	n.a.	lateral
	Kozanek et al., 2009	8 (32 – 49 years)	dual-plane fluoroscopy	stance	TEA GCA	9.7 ± 0.7 mm 17.4 ± 2.0 mm	4.0 ± 1.7 mm 7.4 ± 6.1 mm	n.a. n.a.
	Liu et al., 2010	8 (32 – 49 years)	dual-plane fluoroscopy	stance	CP	3.6 ± 0.3 mm	1.6 ± 0.4 mm	lateral
	Postolka et al., 2020b	10 (23.7 ± 3.2 years)	single-plane fluoroscopy	stance & swing	FFA	stance: 8.3 ± 1.8 mm swing: 6.6 ± 1.6 mm	stance: 8.2 ± 1.4 mm swing: 8.1 ± 1.8 mm	medial
					NP	stance: 10.3 ± 3.2 mm swing: 13.3 ± 4.3 mm	stance: 15.5 ± 6.1 mm swing: 21.7 ± 8.5 mm	n.a.

A-P: antero-posterior, CoR: centre of rotation, RoM: range of motion, a: anterior, p: posterior
GCA: geometric centre axis, FFC: flexion facet centre, EFC: extension facet centre, FFA: functional flexion axis, TEA: transepicondylar axis, NP: nearest point, CP: contact point

calculated as the translation of these points with respect to the tibial anatomical coordinate system. To account for individual knee sizes, all A-P translations were scaled to the average femoral width across all subjects (Postolka et al., 2020b). A-P translations during continuous knee flexion were analysed as a function of tibio-femoral flexion angle, while A–P translations during level walking were temporally normalized to a complete gait cycle. For each approach, the location of the CoR in the transverse plane was calculated using the symmetrical CoR estimation (SCoRe) approach based on the location of the respective medial and lateral points (Ehrig et al., 2006).

2.3. Statistics

Two mixed-model analyses of variances (ANOVAs), one for continuous knee bending and one for level walking, were performed to investigate differences in the ranges of A-P translation between the medial and lateral condyles, as well as the effect of the kinematic analysis approach. The range of A-P translation was set as the dependent variable. Kinematic analysis approach (six levels: FFA, TEA, CA, EFC/FFC, NP, SEP) and condyle (two levels: medial, lateral) were set as fixed effects, with subject as random effect. Post-hoc comparisons were conducted using a least significant difference (LSD) approach, and significance levels were adjusted for multiple comparisons using Bonferroni correction. The ANOVA analysis was conducted using the SPSS software suite (SPSS v24, IBM, USA).

In order to analyse the effects of the different kinematic analysis approaches on A-P translation over the whole time series, one-dimensional statistical parametric mapping (SPM) (Pataky et al., 2016) was performed using the open-source toolbox SPM-1D (Pataky 2017, v.M.0.4.5). For each activity, two one-way ANOVAs were performed, one for each condyle. A-P translation was set as the dependent variable and the kinematic analysis approach (six levels: FFA, TEA, CA, EFC/FFC, NP, SEP) as the independent variable. Post-hoc comparisons were conducted using a two-sample t–test and significance levels were adjusted for multiple comparisons using Bonferroni correction.

3. Results

3.1. Continuous knee bending

Across all subjects and all trials of continuous knee bending, flexion ranged from -10° to 156°. A range of 25° to 115° was covered by all subjects and therefore used for statistical comparison.

For both the ranges as well as patterns of medial and lateral condylar A-P translation, significant differences were found between the different kinematic analysis approaches (Fig. 1, Figure S1). The TEA exhibited significantly larger ranges of condylar translation than all other kinematic analysis approaches for both condyles ($p < 0.001$). In addition, the CA resulted in significantly more condylar translation of the medial condyle than the NP, SEP, FFA, and EFC/FFC ($p < 0.001$) whereas the FFA resulted in the smallest range of A-P translation for the lateral condyle ($p < 0.001$). While the femur fixed axes showed a posterior translation of the medial condyle point after about 50° of flexion, the two contact approaches remained central on the tibial plateau and were located significantly more anteriorly at higher flexion angles than the FFA, TEA and CA ($p < 0.001$, Fig. 1). For the lateral condyle however, all six kinematic analysis approaches showed a tendency towards posterior translation with increasing knee flexion, with the TEA located significantly more posteriorly than the FFA, NP and SEP after 70° ($p < 0.001$, Fig. 1, Table S1).

The FFA ($p = 0.470$) and CA ($p = 0.823$) showed comparable ranges of condylar translation for the medial and lateral condyles and therefore a mean transverse plane CoR located centrally on the tibial plateau (Table 5, Fig. 3, Table S3). In contrast, the TEA, EFC/FFC as well as both contact approaches resulted in significantly larger ranges of A-P translation for the lateral compared to the medial condyle ($p < 0.001$), hence presenting a clear medial CoR (Table 5, Fig. 3, Table S3). However, variability between subjects was high, resulting in opposing translational patterns and a large variation for the mean CoR for certain subjects (Table S2, Table S3).

3.2. Level walking

Similar to continuous knee bending, the ranges and patterns of condylar A-P translation were significantly different between the six kinematic analysis approaches (Table 5, Figure S1. For both condyles,

Table 4
Description of all six kinematic analysis approaches used.

Approach		Definition
Contact Approaches	Nearest Point (NP)	Weighted mean of the ten nearest points of the medial and lateral femoral condyle relative to a plane parallel to the tibial articular surface.
	Tibio-Femoral Separation Point (SEP)	Based on the nearest point of each femoral condyle relative to a plane parallel to the tibial articular surface, a separation threshold was set by adding 6 mm to the nearest point (to account for missing articular cartilage (Moro-oka et al., 2008)). The tibio-femoral separation point was then calculated as the geometric centre of the femoral region with less separation than the threshold.
Functional Axis	Functional Flexion Axis (FFA)	Medio-lateral axis of the femoral anatomical coordinate system, defined based on the relative segmental kinematics of three continuous knee bending trials covering 15 – 90° of flexion and calculated using the symmetrical axis of rotation approach (SARA) (Ehrig et al., 2007).
Anatomical Axes	Transepicondylar Axis (TEA)	The most prominent medial and lateral epicondylar regions were manually selected from the segmented femoral surfaces using the Rhinoceros software (Rhinoceros v5, Robert McNeel & Associates). The medial and lateral epicondylar points (mean of all selected surface points) were connected to form the anatomical TEA.
	Cylinder Axis (CA)	Cylinders on each of the medial and lateral condylar surfaces were defined that intersected the most distal (lowest) point of each femoral condyle (in the sagittal plane). The CA was defined as the common axis of the two cylinders.
	Extension Facet Centre (EFC) & Flexion Facet Centre (FFC)	Based on the location of the nearest points during standing, deep knee bending and level walking, the corresponding surface points on the medial and lateral condyles were extracted at maximum extension, 20° and 120° flexion. The surface points between the point at maximal extension and 20° flexion were used to fit an extension circle, while the surface points at 20° and 120° flexion were used to fit a flexion circle. The circles were fitted using the approach suggested by Taubin (1991), with the anatomical medio-lateral axis set as the normal axis of the fitted circles. The centres of the circles were used as the extension facet centres and flexion facet centres. Due to the absence of knee extension in one subject in our study, no extension facet centres could be detected and therefore EFC/FFC was not analysed for this subject.

the FFA resulted in similar ranges of A-P translation when compared with the CA ($p = 0.078/p = 0.120$), but exhibited significantly smaller ranges than the other four kinematic analysis approaches (TEA, EFC/FFC, NP, SEP, $p < 0.001$). Over the complete gait cycle, significant differences were found during the stance phase and the end of the swing phase (Figure S1). For the medial condyle, all six kinematic analysis approaches showed similar translational patterns during the loaded stance phase with the two contact approaches (NP & SEP) being located significantly more anteriorly than the FFA and CA ($p < 0.001$). During the unloaded swing phase, the medial condyle showed a rapid posterior translation followed by an anterior translation for all six kinematic analysis approaches (Fig. 2, Table S1). While the FFA, CA and TEA showed similar translational patterns for the lateral condyle, the contact approaches (NP & SEP) as well as the EFC/FFC showed different patterns of translation. The NP and SEP resulted in more anterior locations of the lateral condyle compared to the FFA and CA, especially during the second half of the swing phase. In addition, the TEA was located significantly more anteriorly than the FFA ($p < 0.001$, Fig. 2, Table S1).

Over the complete gait cycle of level walking, the lateral condyle experienced significantly more A-P translation than the medial condyle for all six kinematic analysis approaches ($p < 0.001$), resulting in an overall medial position of the CoR in the transverse plane (Fig. 3, Table S3).

4. Discussion

A clear understanding of tibio-femoral kinematics is a prerequisite before consensus can be found on the interpretation of joint functionality and treatment outcomes. This study compared medial and lateral condylar A-P translations of identical kinematic data but based on six kinematic analysis approaches in order to understand their differences and initiate discussion on how tibio-femoral kinematics should best be reported. Our results, based on dynamic videofluoroscopy data of ten healthy subjects during multiple trials of continuous knee bending as well as complete cycles of level walking, demonstrated significant differences between the reported A-P translations and the location of the overall CoR using the different kinematic analysis approaches.

The femur fixed axis approaches (FFA, TEA, CA & EFC/FFC) generally resulted in comparable condylar translations, especially at low flexion angles. The contact estimations (NP & SEP), however, exhibited different translational patterns and were located significantly more anteriorly than most femur fixed axes (Fig. 1, Fig. 2). These dissimilarities resulting from methodology alone could plausibly explain some of the different interpretations of joint kinematics described in the literature:

Continuous knee bending: Comparable to existing data, the femur fixed axes showed a trend towards initial anterior followed by posterior translation of the medial condyle, whereas the lateral condyle translated continuously posteriorly (Fig. 1) (Asano et al., 2001; Tanifuji et al., 2013, 2011; Zhou et al., 2021). In contrast to the general translational patterns, the RoM for the TEA and geometric centre axis (GCA) slightly varied from values previously published, most likely due to the differences in the flexion range analysed (Asano et al., 2001; Tanifuji et al., 2013, 2011). For the associated tibio-femoral rotations, a medial CoR reported in the literature for flexions from 0° to 120°/140° (Asano et al., 2001; Tanifuji et al., 2013, 2011), was only found using the TEA but not the CA in the current study (Fig. 3). Translations using the medial and lateral contact approaches (NP & SEP) presented similar trends to previous studies, indicating more translation on the lateral than the medial side (DeFrate et al., 2004; Dennis et al., 2005; Grieco et al., 2018; Hamai et al., 2013; Komistek et al., 2003; Li et al., 2006), but two studies (Pinskerova et al., 2004; Qi et al., 2013) examining the contact location have also presented equal translations of both condyles, which could not be replicated within the present study. This is most likely due to the fact that these studies assessed contact location based on the articular cartilage distance measured using MRI (Pinskerova et al., 2004; Qi et al.,

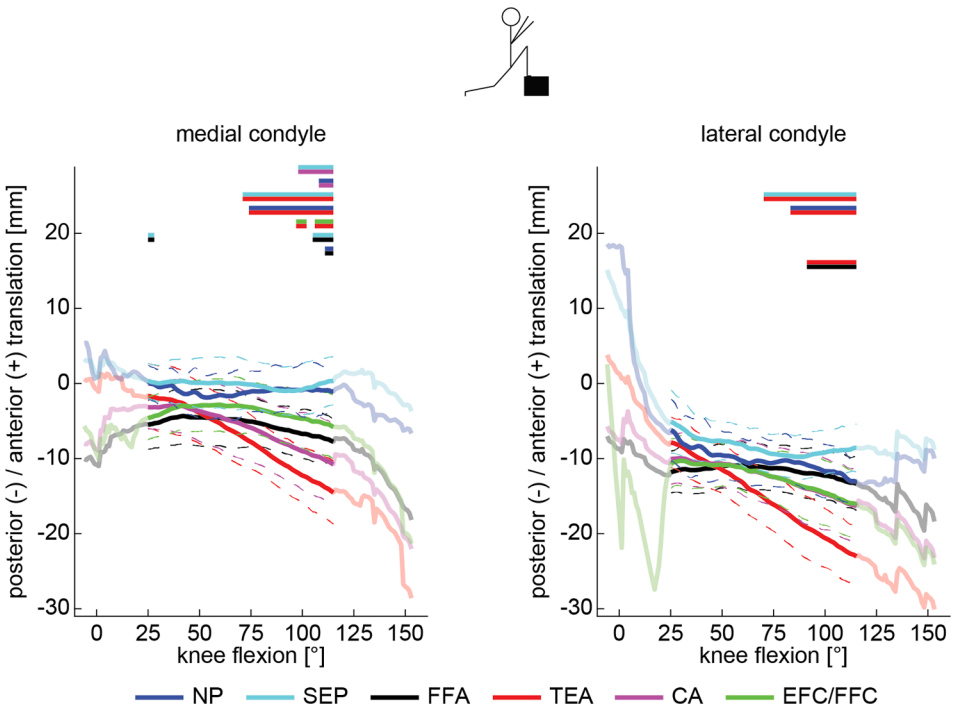

Fig. 1. Antero-posterior translation of the medial (left) and lateral (right) condyle using the nearest point (NP), tibio-femoral separation (SEP), functional flexion axis (FFA), transepicondylar axis (TEA), cylinder axis (CA), and extension facet centres/flexion facet centres (EFC/FFC) during continuous knee bending are shown as a function of the flexion angle. Mean (thick line) and standard deviations (dashed line) across all 10 subjects are presented. Light coloured lines indicate the mean across subjects for flexion angles that were not covered by all subjects. Significant differences between approaches are indicated with bars in the colours of the respective approaches with an adjusted level of significance of $\alpha = 0.0033$.

Table 5
Range of antero-posterior (A-P) translation (mean ± standard deviation) of the medial and lateral condyle during continuous knee bending and level walking using the nearest point (NP), tibio-femoral separation (SEP), functional flexion axis (FFA), transepicondylar axis (TEA), cylinder axis (CA), and extension facet centres/flexion facet centres (EFC/FFC). In addition, the resultant p-value of the performed ANOVA to investigate differences in the range of A-P translation between the medial and lateral condyle for each approach is indicated.

RoM [mm]	NP	SEP	FFA	TEA	CA	EFC/FFC
continuous knee bending						
medial condyle	5.7 ± 1.2	4.2 ± 0.8	4.8 ± 1.5	13.8 ± 5.4	9.1 ± 3.9	5.2 ± 1.8
lateral condyle	9.8 ± 2.2	7.6 ± 2.3	5.2 ± 1.3	16.1 ± 2.8	9.2 ± 3.1	9.0 ± 1.9
resultant p-value	*<0.001**	*<0.001**	*0.470*	*<0.001**	*0.823*	*<0.001**
level walking (complete gait cycle)						
medial condyle	14.7 ± 3.4	11.1 ± 2.7	8.0 ± 1.4	12.1 ± 2.5	9.7 ± 2.9	11.7 ± 3.6
lateral condyle	25.4 ± 5.6	19.5 ± 4.1	11.0 ± 1.8	17.2 ± 3.6	12.6 ± 3.3	27.8 ± 12.9
resultant p-value	*<0.001**	*<0.001**	*<0.001**	*<0.001**	*0.001**	*<0.001**

** significant difference on an adjusted level of significance of $\alpha = 0.0083$*

2013). Overall, the missing statistical analysis of extension (knee flexion < 25°) and deep knee flexion (knee flexion > 115°) limited the comparison to previous published studies.

Level walking: Over the complete gait cycle, our results regarding the extent of tibio-femoral translation but also the relative differences between the medial and lateral condyles using the CA (medial: 9.7 mm; lateral: 12.6 mm) are in line with translations reported using a GCA (medial: 7.6 mm; lateral: 11.6 mm) (Gray et al., 2019). However, contradictory results have been reported for the loaded stance phase: We observed posterior translation of both condyles during early stance and in preparation for the swing phase, as well as a greater range of translation of the lateral over the medial condyle (using CA & TEA, Fig. 2, Table 5). Here, Kozanek and co-workers (2009) reported an initial anterior peak during early stance, and again anterior translation of the medial condyle prior to toe-off (GCA: 17.4 mm; TEA: 9.7 mm), with only limited translation of the lateral condyle until late stance, followed by anterior translation in pre-swing (GCA: 7.4 mm; TEA: 4.0 mm). Our results also indicate more A-P translation for both condyles than presented in the literature when using contact approaches (Dennis et al., 2001; Gray et al., 2019; Komistek et al., 2003; Liu et al., 2010). In particular, we observed large inter-subject differences in the location of the lateral NP during the stance phase, which is previously unreported.

Overall, it is likely that each of the kinematic analysis approaches presented in this study represents different aspects of tibio-femoral motion, and differences between femur fixed axes and contact estimates are therefore entirely conceivable (Nakamura et al., 2015). Femur fixed axes (FFA, TEA, CA & EFC/FFC) are able to provide information on the relative positions of the femur and tibia. However, it is well accepted that the knee exhibits both rolling and gliding motions that are associated with the complex interaction of tibio-femoral rotations and translations. Pure femoral gliding (i.e. rotation with sliding at the articulating interface) clearly leads to an axis of rotation that is consistent with the condylar geometry. The difficulty, however, arises when rolling occurs (no slippage at the joint surface). Here, the instantaneous axis of rotation moves distally towards the articulating contact interface between the tibia and femur. Any deviations of femur fixed axes from the instantaneous axis of rotation (e.g. as the anatomical points rotate about the true axis) will directly lead to kinematic crosstalk between flexion and translation (Fig. 4A). As a result, any segment fixed axis might be able to correctly reconstruct relative segment motion at certain instances (whenever the axis coincides with the true axis of rotation) but will introduce translational crosstalk over the remaining majority of the movement cycle. In the current study, the TEA and CA were located anteriorly of the FFA during lower but posteriorly at higher flexion

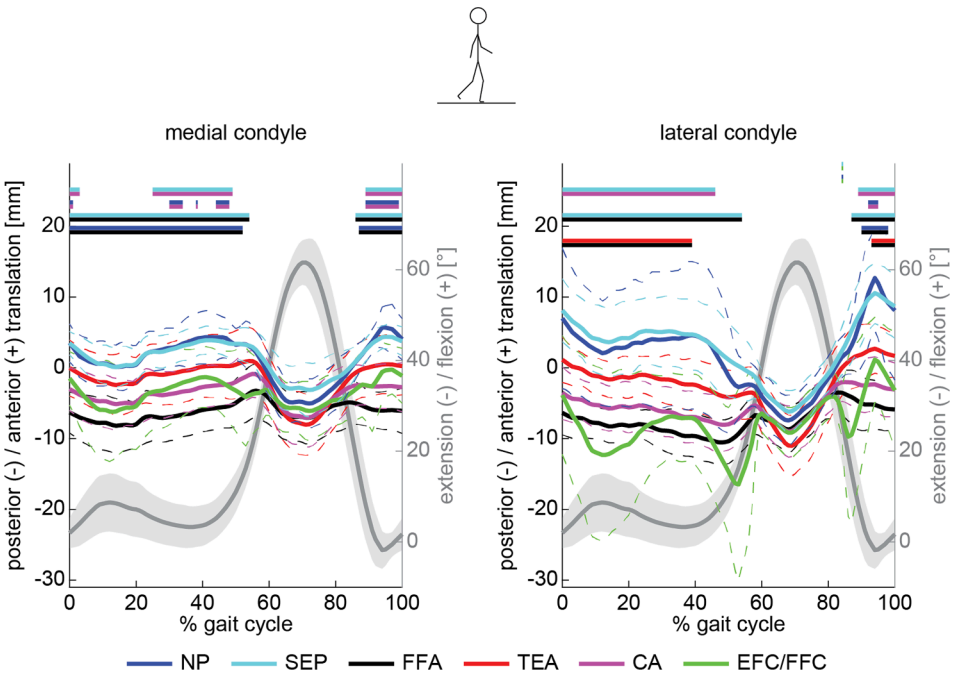

Fig. 2. Antero-posterior translation of the medial (left) and lateral (right) condyle using the nearest point (NP), tibio-femoral separation (SEP), functional flexion axis (FFA), transepicondylar axis (TEA), cylinder axis (CA), and extension facet centres/flexion facet centres (EFC/FFC) over a complete gait cycle of level walking. Mean (thick line) and standard deviations (dashed line) across all 10 subjects are presented. In addition, the mean (grey thick line) and standard deviation (grey shaded area) of the knee flexion angle is indicated. Significant differences between approaches are indicated with bars in the colours of the respective approaches with an adjusted level of significance of $\alpha = 0.0033$.

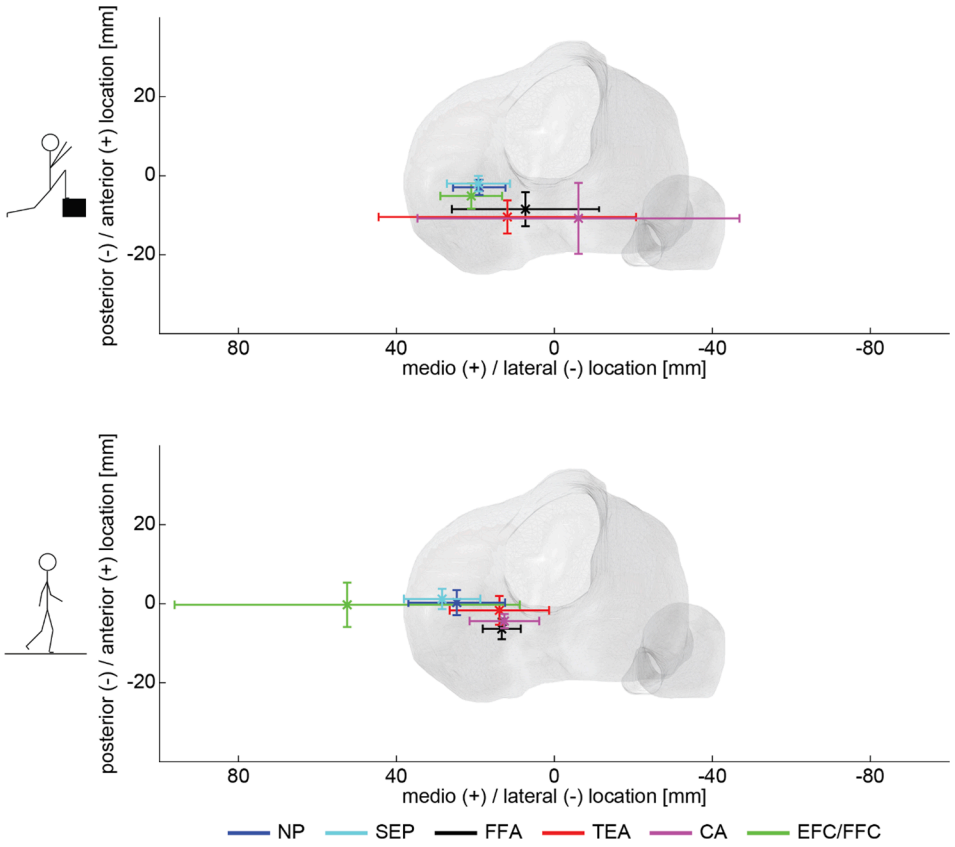

Fig. 3. Location of the centre of rotation shown on the tibial plateau during continuous knee bending (top) and complete cycle of level walking (bottom) using the nearest point (NP), tibio-femoral separation (SEP), functional flexion axis (FFA), transepicondylar axis (TEA), cylinder axis (CA), and extension facet centres/flexion facet centres (EFC/FFC). The mean across all 10 subjects as well as the standard deviations in antero-posterior and medio-lateral directions are indicated with whiskers.

angles (Fig. 1), highlighting the crosstalk effect through clear coupling between condylar translation and knee flexion angle (Fig. 4B). Within this study, the FFA was optimised over 15° to 90° of knee flexion in three continuous knee bending trials (Ehrig et al., 2007), and thus thought to approximate to the instantaneous axis of rotation and therefore likely to be least affected by kinematic crosstalk. Here, it is important to note that the FFA is solely defined based on a calibration movement without any subjective input. The anatomical axes, however, require initial definition of anatomical landmarks (TEA), planes (CA & EFC/FFC), and sections of the condylar surface (EFC/FFC) by the observer and could therefore introduce subjective bias.

Contact point approaches on the other hand can offer information of

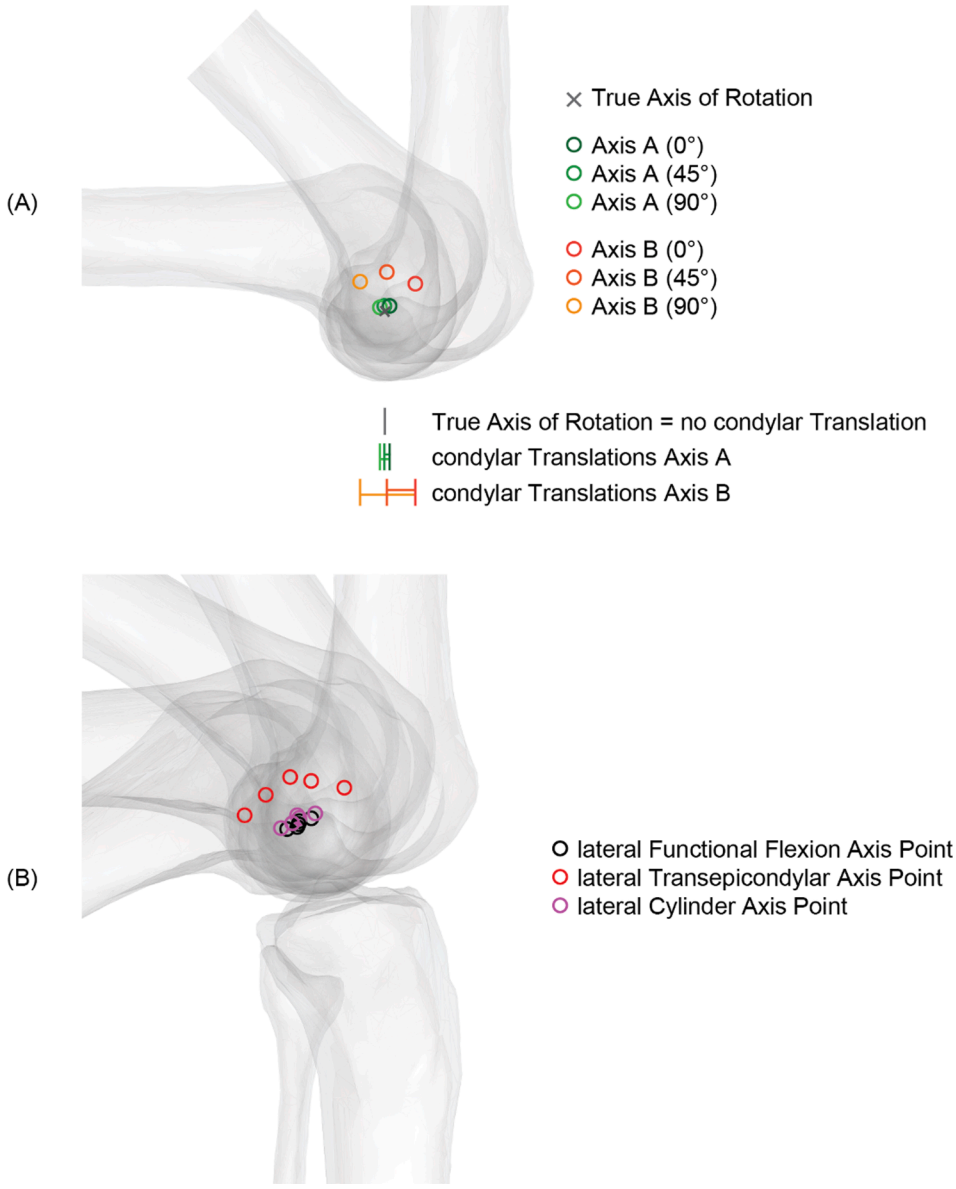

Fig. 4. (A) Schematic image of the femur rotating in a tibial coordinate system, with the true axis of rotation shown as grey x. The representation shows the movement of two different femur fixed axis (Axis A & Axis B) at three different flexion angles, as well as the associated condylar translations relative to the initial position. The graphic demonstrates the potential for false interpretation of condylar translation that is, in fact, only an artefact of rotation around the true axis of rotation. (B) Real data from our study showing the location of the femur relative to the tibia during a continuous knee bending trial at 0°, 30°, 60°, 90° and 120° of flexion. The location of the lateral functional flexion axis point, the lateral transepicondylar axis point, and the lateral cylinder axis point are indicated for each flexion angle. Since the movement data analysed was consistent throughout, these results demonstrate the potential for conflicting interpretations of joint kinematics resulting from the kinematic analysis approach used.

localized contact conditions at the condylar surfaces. Importantly, these approaches are not affected by kinematic crosstalk with progressive flexion, but are particularly sensitive to femoral and tibial anatomy. Within this study, a few subjects exhibited a relatively flat lateral femoral condyle leading to "jumps" of the NP during phases of knee extension and thus resulting in large inter-subject variability (Iwaki et al., 2000; Postolka et al., 2020b). Of note, contact approaches can either use a plane to represent the tibial surface, which loses sensitivity to the local mechanical conditions, or use realistic anatomical conditions, which are extremely sensitive to the accuracy of the kinematic data. Options to overcome such sensitivities include the analysis of overlapping cartilage regions (DeFrate et al., 2004).

Within the current study, a central to medial CoR was found using all six kinematic analysis approaches in both continuous knee bending and level walking (Fig. 3), even though some individuals did indeed exhibit a lateral CoR when analysed using certain kinematic analysis approaches (Table S3). While studies reporting a lateral CoR during walking have generally used contact-based approaches (Koo and Koo, 2019; Kozanek et al., 2009), we have been unable to replicate these results. These findings suggest that factors other than the kinematic analysis approach also play a role in the differences found among the published literature. Therefore, more research is needed to gain a detailed understanding of the influence of subject-specific anatomy, including soft-tissue structures, or individual movement strategies on the resulting tibio-femoral kinematics.

While the present study could clearly demonstrate the effect of various kinematic analysis approaches at different flexion angles or phases of a functional activity, despite the assessment of identical tibio-femoral kinematics, there were obvious limitations to our study. Due to large inter-subject differences in the range of flexion covered during continuous knee bending, statistical analysis of phases low (<25°) as well as deep knee flexion (>115°) are missing. Although the single-plane fluoroscopy set-up is limited in out-of-plane accuracy, the data presented here was based on the position of the femur relative to a plane parallel to the tibial articular surface and therefore mainly affected by the in-plane translational and rotational error (<0.6 mm/<1°) (Postolka et al., 2020a). Finally, in subjects exhibiting on average a parallel translational movement pattern (i.e. equal translation of the medial and lateral condyle points), calculation of the CoR was only partially robust, resulting in large intra-subject variability for the CoR M–L location, and hence large standard deviations of up to 40.3 mm were observed for a single subject (Table S2, Table S3).

Overall, this study clearly demonstrated that the reported tibio-femoral kinematics are sensitive to the kinematic analysis approach used. In comparison with previously reported condylar translations, our results were remarkably similar when using the same kinematic analysis approach, especially during the more standardised continuous knee bending. Conversely, our data for walking was less in agreement with previous studies, even when using the same kinematic analysis approaches, suggesting that the approach alone cannot explain all of the differences in tibio-femoral kinematics observed. To quantify knee joint functionality and further evaluate outcome differences, it is therefore critical that the biomechanics community reaches consensus on when each specific kinematic analysis approach should best be used in order to exclude any bias in method related interpretation of joint kinematics. While anatomical axes offer the advantage of comparison against considerable previous work in this area, we recommend that joint translations should be reported using functional flexion axes in preference to anatomical axes in order to minimise subjective bias and reduce the effect of cross-talk. In addition, presenting contact points can contribute valuable information to the localized contact conditions at the condylar surfaces, and should therefore be reported to inform on questions addressing loading, overloading, and/or wear at the joint. Reporting tibio-femoral kinematics using at least two different kinematic analysis approaches would hence allow a more standardised comparison and interpretation of different subject populations and activities.

CRediT authorship contribution statement

Barbara Postolka: Visualization, Methodology, Investigation, Formal analysis, Data curation, Conceptualization, Writing - original draft, Writing - review & editing. **William R. Taylor:** Supervision, Resources, Project administration, Funding acquisition, Conceptualization, Writing - original draft, Writing - review & editing. **Katrin Dätwyler:** Methodology, Formal analysis, Data curation, Writing - review & editing. **Markus O. Heller:** Methodology, Conceptualization, Writing - review & editing. **Renate List:** Resources, Project administration, Methodology, Funding acquisition, Conceptualization, Writing - review & editing. **Pascal Schütz:** Supervision, Resources, Project administration, Methodology, Investigation, Funding acquisition, Formal analysis, Data curation, Conceptualization, Writing - original draft, Writing - review & editing.

Declaration of Competing Interest

The authors declare that they have no known competing financial interests or personal relationships that could have appeared to influence the work reported in this paper.

Acknowledgements

This project was partially funded by Medacta International SA (Castel San Pietro, Switzerland) and the Commission for Technology and Innovation (Bern, Switzerland, Project Number 17078.1 PFLS-LS). The sponsor was not involved in the data collection, nor in the analysis or the interpretation of the data. Furthermore, the authors would like to thank Maryam Hajizadeh for her initial work in comparing different kinematic analysis approaches.

Appendix A. Supplementary data

Supplementary data to this article can be found online at https://doi.org/10.1016/j.jbiomech.2022.111306.

References

Andriacchi, T.P., Alexander, E.J., Toney, M.K., Dyrby, C., Sum, J., 1998. A point cluster method for in vivo motion analysis: applied to a study of knee kinematics. J. Biomech. Eng. 120, 743–749.
Asano, T., Akagi, M., Tanaka, K., Tamura, J., Nakamura, T., 2001. In vivo three-dimensional knee kinematics using a biplanar image-matching technique. Clin. Orthop. Relat. Res. 157–166.
Asano, T., Akagi, M., Nakamura, T., 2005. The functional flexion-extension axis of the knee corresponds to the surgical epicondylar axis: in vivo analysis using a biplanar image-matching technique. J. Arthroplast. 20, 1060–1067.
Banks, S.A., Banks, A.Z., Cook, F.F., Hodge, W.A., 1996. Markerless three dimensional measurement of knee kinematics using single-plane fluoroscopy. 20th Annu. Meet. Am. Soc. Biomech.
Banks, S.A., Hodge, W.A., 2004. 2003 Hap Paul Award Paper of the International Society for Technology in Arthroplasty. Design and activity dependence of kinematics in fixed and mobile-bearing knee arthroplasties. J. Arthroplast. 19, 809–816.
Berger, R.A., Rubash, H.E., Seel, M.J., Thompson, W.H., Crossett, L.S., 1993. Determining the rotational alignment of the femoral component in total knee arthroplasty using the epicondylar axis. Clin. Orthop. Relat. Res. 40–47.
Besier, T.F., Sturnieks, D.L., Alderson, J.A., Lloyd, D.G., 2003. Repeatability of gait data using a functional hip joint centre and a mean helical knee axis. J. Biomech. 36, 1159–1168.
Churchill, D.L., Incavo, S.J., Johnson, C.C., Beynnon, B.D., 1998. The transepicondylar axis approximates the optimal flexion axis of the knee. Clin. Orthop. Relat. Res. 111–118.
DeFrate, L.E., Sun, H., Gill, T.J., Rubash, H.E., Li, G., 2004. In vivo tibiofemoral contact analysis using 3D MRI-based knee models. J. Biomech. 37, 1499–1504.
Dennis, D.A., Komistek, R.D., Scuderi, G.R., Argenson, J.-N., Insall, J., Mafouz, M., Aubaniac, J.-M., Haas, B., 2001. In vivo three-dimensional determination of kinematics for subjects with a normal knee or a unicompartmental or total knee replacement. J. Bone Jt. Surg. Am. 83-A Suppl, 104–115.
Dennis, D.A., Mahfouz, M.R., Komistek, R.D., Hoff, W., 2005. In vivo determination of normal and anterior cruciate ligament-deficient knee kinematics. J. Biomech. 38, 241–253.
Eckhoff, D.G., Dwyer, T.F., Bach, J.M., Spitzer, V.M., Reinig, K.D., 2001. Three-dimensional morphology of the distal part of the femur viewed in virtual reality. J. Bone Jt. Surg. Am. 83-A Suppl, 43–50.
Eckhoff, D., Hogan, C., DiMatteo, L., Robinson, M., Bach, J., 2007. Difference between the epicondylar and cylindrical axis of the knee. Clin. Orthop. Relat. Res. 461, 238–244.
Ehrig, R.M., Heller, M.O., 2019. On intrinsic equivalences of the finite helical axis, the instantaneous helical axis, and the SARA approach. A mathematical perspective. J. Biomech. 84, 4–10.
Ehrig, R.M., Taylor, W.R., Duda, G.N., Heller, M.O., 2006. A survey of formal methods for determining the centre of rotation of ball joints. J. Biomech. 39, 2798–2809.
Ehrig, R.M., Taylor, W.R., Duda, G.N., Heller, M.O., 2007. A survey of formal methods for determining functional joint axes. J. Biomech. 40, 2150–2157.
Feng, Y., Tsai, T.Y., Li, J.S., Rubash, H.E., Li, G., Freiberg, A., 2016. In-vivo analysis of flexion axes of the knee: Femoral condylar motion during dynamic knee flexion. Clin. Biomech. 32, 102–107.
Freeman, M.A.R., Pinskerova, V., 2005. The movement of the normal tibio-femoral joint. J. Biomech. 38, 197–208.
Galvin, C.R., Perriman, D.M., Lynch, J.T., Pickering, M.R., Newman, P., Smith, P.N., Scarvell, J.M., 2019. Age has a minimal effect on knee kinematics: A cross-sectional 3D/2D image-registration study of kneeling. Knee 26, 988–1002.
Gamage, S.S., Lasenby, J., 2002. New least squares solutions for estimating the average centre of rotation and the axis of rotation. J. Biomech. 35, 87–93.
Gray, H.A., Guan, S., Thomeer, L.T., Schache, A.G., de Steiger, R., Pandy, M.G., 2019. Three-dimensional motion of the knee-joint complex during normal walking revealed by mobile biplane X-ray imaging. J. Orthop. Res. 37, 615–630.
Grieco, T.F., Sharma, A., Dessinger, G.M., Cates, H.E., Komistek, R.D., 2018. In Vivo Kinematic Comparison of a Bicruciate Stabilized Total Knee Arthroplasty and the Normal Knee Using Fluoroscopy. J. Arthroplast. 33, 565–571.
Guan, S., Gray, H.A., Keynejad, F., Pandy, M.G., 2016. Mobile Biplane X-Ray Imaging System for Measuring 3D Dynamic Joint Motion During Overground Gait. IEEE Trans. Med. Imaging 35, 326–336.
Hamai, S., Moro-oka, T.A., Dunbar, N.J., Miura, H., Iwamoto, Y., Banks, S.A., 2013. In vivo healthy knee kinematics during dynamic full flexion. Biomed Res. Int. 2013, 717546.
Hill, P.F., Vedi, V., Williams, A., Iwaki, H., Pinskerova, V., Freeman, M.A., 2000. Tibiofemoral movement 2: the loaded and unloaded living knee studied by MRI. J. Bone Jt. Surg. Br. 82, 1196–1198.
Holzreiter, S., 1991. Calculation of the instantaneous centre of rotation for a rigid body. J. Biomech. 24, 643–647.
Iwaki, H., Pinskerova, V., Freeman, M.A.R., 2000. Tibiofemoral movement 1: the shapes and relative movements of the femur and tibia in the unloaded cadaver knee. J. Bone Jt. Surg. Br. 82, 1189–1195.
Johal, P., Williams, A., Wragg, P., Hunt, D., Gedroyc, W., 2005. Tibio-femoral movement in the living knee. A study of weight bearing and non-weight bearing knee kinematics using "interventional" MRI. J. Biomech. 38, 269–276.
Komistek, R.D., Dennis, D.A., Mahfouz, M., 2003. In vivo fluoroscopic analysis of the normal human knee. Clin. Orthop. Relat. Res. 69–81.
Koo, Y.J., Koo, S., 2019. Three-dimensional kinematic coupling in the knee during normal walking. J. Biomech. Eng. 141, 81012.

Kozanek, M., Hosseini, A., Liu, F., Van de Velde, S.K., Gill, T.J., Rubash, H.E., Li, G., 2009. Tibiofemoral kinematics and condylar motion during the stance phase of gait. J. Biomech. 42, 1877–1884.
Kurosawa, H., Walker, P.S., Abe, S., Garg, A., Hunter, T., 1985. Geometry and motion of the knee for implant and orthotic design. J. Biomech. 18, 487–499.
Li, G., DeFrate, L.E., Park, S.E., Gill, T.J., Rubash, H.E., 2005. In vivo articular cartilage contact kinematics of the knee: an investigation using dual-orthogonal fluoroscopy and magnetic resonance image-based computer models. Am. J. Sport. Med. 33, 102–107.
Li, G., Moses, J.M., Papannagari, R., Pathare, N.P., DeFrate, L.E., Gill, T.J., 2006. Anterior cruciate ligament deficiency alters the in vivo motion of the tibiofemoral cartilage contact points in both the anteroposterior and mediolateral directions. J. Bone Jt. Surg. Am. 88a, 1826–1834.
Li, G., Van de Velde, S.K., Bingham, J.T., 2008. Validation of a non-invasive fluoroscopic imaging technique for the measurement of dynamic knee joint motion. J. Biomech. 41, 1616–1622.
List, R., Postolka, B., Schütz, P., Hitz, M., Schwilch, P., Gerber, H., Ferguson, S.J., Taylor, W.R., 2017. A moving fluoroscope to capture tibiofemoral kinematics during complete cycles of free level and downhill walking as well as stair descent. PLoS ONE 12.
Liu, F., Kozanek, M., Hosseini, A., Van de Velde, S.K., Gill, T.J., Rubash, H.E., Li, G., 2010. In vivo tibiofemoral cartilage deformation during the stance phase of gait. J. Biomech. 43, 658–665.
Moro-oka, T.A., Hamai, S., Miura, H., Shimoto, T., Higaki, H., Fregly, B.J., Iwamoto, Y., Banks, S.A., 2008. Dynamic activity dependence of in vivo normal knee kinematics. J. Orthop. Res. 26, 428–434.
Most, E., Axe, J., Rubash, H., Li, G., 2004. Sensitivity of the knee joint kinematics calculation to selection of flexion axes. J. Biomech. 37, 1743–1748.
Nakamura, S., Sharma, A., Ito, H., Nakamura, K., Zingde, S.M., Komistek, R.D., 2015. Kinematic difference between various geometric centers and contact points for tri-condylar Bi-surface knee system. J Arthroplast. 30, 701–705.
Pataky, T.C., Robinson, M.A., Vanrenterghem, J., 2016. Region-of-interest analyses of one-dimensional biomechanical trajectories: bridging 0D and 1D theory, augmenting statistical power. PeerJ 4.
Pauchard, Y., Fitze, T., Browarnik, D., Eskandari, A., Pauchard, I., Enns-Bray, W., Palsson, H., Sigurdsson, S., Ferguson, S.J., Harris, T.B., Gudnason, V., Helgason, B., 2016. Interactive graph-cut segmentation for fast creation of finite element models from clinical ct data for hip fracture prediction. Comput. Methods Biomech. Biomed. Eng. 19, 1693–1703.
Pinskerova, V., Johal, P., Nakagawa, S., Sosna, A., Williams, A., Gedroyc, W., Freeman, M.A., 2004. Does the femur roll-back with flexion? J. Bone Jt Surg. Br. 86, 925–931.
Postolka, B., List, R., Thelen, B., Schütz, P., Taylor, W.R., Zheng, G., 2020. Evaluation of an intensity-based algorithm for 2D/3D registration of natural knee videofluoroscopy data. Med. Eng. Phys. 77, 107–113.
Postolka, B., Schütz, P., Fucentese, S.F., Freeman, M.A.R., Pinskerova, V., List, R., Taylor, W.R., 2020. Tibio-femoral kinematics of the healthy knee joint throughout complete cycles of gait activities. J. Biomech. 110.
Qi, W., Hosseini, A., Tsai, T.Y., Li, J.S., Rubash, H.E., Li, G.A., 2013. In vivo kinematics of the knee during weight bearing high flexion. J. Biomech. 46, 1576–1582.
Schütz, P., Taylor, W.R., Postolka, B., Fucentese, S.F., Koch, P.P., Freeman, M.A.R., Pinskerova, V., List, R., 2019. Kinematic Evaluation of the GMK Sphere Implant during Gait Activities: A Dynamic Videofluoroscopy Study. J. Orthop. Res. 37, 2337–2347.
Tanifuji, O., Sato, T., Kobayashi, K., Mochizuki, T., Koga, Y., Yamagiwa, H., Omori, G., Endo, N., 2011. Three-dimensional in vivo motion analysis of normal knees using single-plane fluoroscopy. J. Ortho Sci. 16, 710–718.
Tanifuji, O., Sato, T., Kobayashi, K., Mochizuki, T., Koga, Y., Yamagiwa, H., Omori, G., Endo, N., 2013. Three-dimensional in vivo motion analysis of normal knees employing transepicondylar axis as an evaluation parameter. Knee Surg. Sport. Traumatol. Arthrosc. 21, 2301–2308.
Taubin, G., 1991. Estimation of Planar Curves, Surfaces, and Nonplanar Space-Curves Defined by Implicit Equations with Applications to Edge and Range Image Segmentation. IEEE Trans. Pattern. Anal. Mach. Intell. 13 (11), 1115–1138.
Vedi, V., Williams, A.M., Tennant, S.J., Spouse, E., Hunt, D.M., Gedroyc, W.M.W., 1999. Meniscal movement. An in-vivo study using dynamic MRI. J. Bone Jt. Surg. Br. 81, 37–41.
Walker, P.S., Heller, Y., Yildirim, G., Immerman, I., 2011. Reference axes for comparing the motion of knee replacements with the anatomic knee. Knee 18, 312–316.
Yamaguchi, S., Gamada, K., Sasho, T., Kato, H., Sonoda, M., Banks, S.A., 2009. In vivo kinematics of anterior cruciate ligament deficient knees during pivot and squat activities. Clin. Biomech. 24, 71–76.
Zhou, C., Zhang, Z., Rao, Z., Foster, T., Bedair, H., Li, G., 2021. Physiological articular contact kinematics and morphological femoral condyle translations of the tibiofemoral joint. J. Biomech. 123.